Tropical Plants

ARTICLE

Open Access

https://doi.org/10.48130/tp-0026-0010

Tropical Plants **2026**, 5: e011

Evolutionary dynamics of pyrethroid resistance in the *Megalurothrips usitatus* of Hainan and detection of voltage-gated sodium channel mutation sites

Authors

Guoliang Xia, Dongfu Yuan, Likui Wang, Ruibo Gao, Qinglong Wang, ..., Shaoying Wu*

Correspondence

wsywsy6000@hainanu.edu.cn (Wu S)

In Brief

From 2024 to 2026, four Hainan *Megalurothrips usitatus* populations were monitored for resistance to three pyrethroids: resistance rose consistently, yet slowed in 2026. T929I was the only resistance mutation with a yearly declining frequency; M918L/T and L1014F were undetected but pose potential risks due to thrips' reproductive traits and their wide presence in related thrips. This study underpins pest resistance monitoring and control.

Graphical abstract

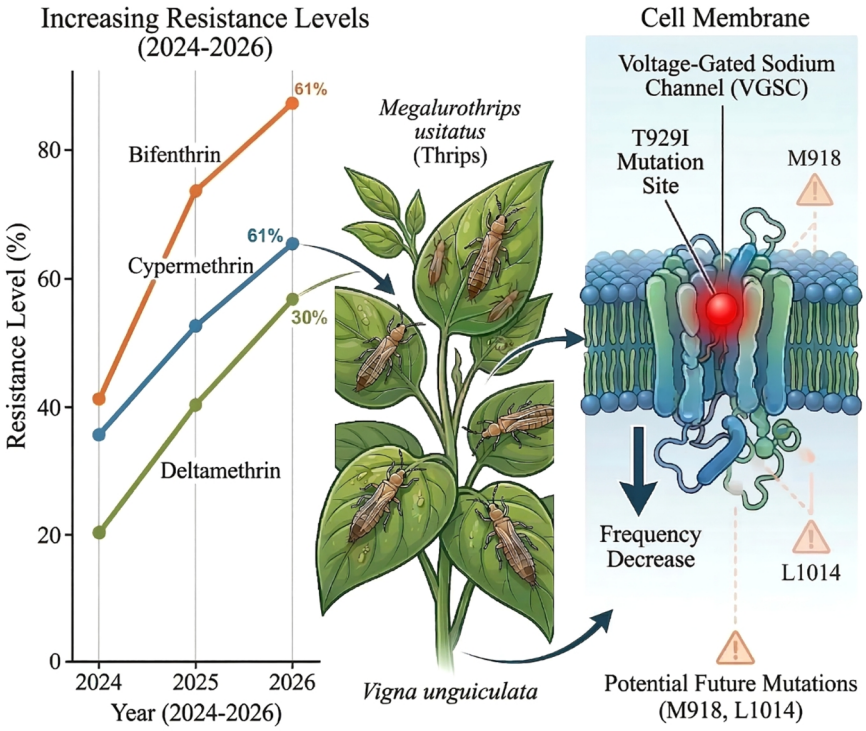

Highlights

- Three-year spatiotemporal dynamics of pyrethroid resistance in *Megalurothrips usitatus* in Hainan were first revealed, filling the gap in long-term resistance monitoring in tropical regions.
- T929I was identified as the only core resistance mutation, while classic kdr/super-kdr mutations were absent, suggesting novel resistance mechanisms in the VGSC.
- Resistance selectivity and geographic differentiation were clarified, supporting rational insecticide application; VGSC cloning and 3D modeling laid a foundation for functional studies and sustainable control.

Citation: Xia G, Yuan D, Wang L, Gao R, Wang Q, et al. 2026. Evolutionary dynamics of pyrethroid resistance in the *Megalurothrips usitatus* of Hainan and detection of voltage-gated sodium channel mutation sites. *Tropical Plants* 5: e011 https://doi.org/10.48130/tp-0026-0010

Tropical Plants

ARTICLE

Open Access

https://doi.org/10.48130/tp-0026-0010

Tropical Plants **2026**, 5: e011

Evolutionary dynamics of pyrethroid resistance in the *Megalurothrips usitatus* of Hainan and detection of voltage-gated sodium channel mutation sites

Guoliang Xia[1,2], Dongfu Yuan[1,2], Likui Wang[1,2], Ruibo Gao[1,2], Qinglong Wang[1,2], Yuran Xie[1,2], Jiang Wayne[3] and Shaoying Wu[1,2,4*]

[1] *School of Breeding and Multiplication (Sanya Institute of Breeding and Multiplication), Hainan University, Sanya, Hainan 572025, China*
[2] *School of Tropical Agriculture and Forestry, Hainan University, Danzhou, Hainan 571737, China*
[3] *Department of Entomology, Michigan State University, East Lansing, MI 48824, USA*
[4] *School of tropical fruits and vegetables, Hainan University, Baoting, Hainan 572300, China*
* Correspondence: wsywsy6000@hainanu.edu.cn (Wu S)

Abstract

To elucidate the evolutionary dynamics and molecular mechanisms underlying resistance to pyrethroid insecticides in the *Megalurothrips usitatus* of Hainan Province, resistance levels to deltamethrin, bifenthrin, and cypermethrin were systematically assessed in four field populations from 2024 to 2026. The voltage-gated sodium channel (VGSC) gene was cloned, and resistance-associated mutation sites were identified. The findings indicated that all four field populations demonstrated elevated levels of resistance to the three pyrethroids. Although resistance continued to escalate from 2024 to 2026, the rate of increase decelerated in 2026. The overall resistance of the populations was ranked as CM-R > LS-R > SY-R > LD-R, with the selectivity of resistance to the insecticides ordered as bifenthrin > cypermethrin > deltamethrin. The full-length VGSC gene of *M. usitatus*, the T929I mutation, was identified in all four field populations, exhibiting a frequency of 100% in 2024. From 2025 to 2026, this frequency exhibited a declining trend, accompanied by population differentiation. Although no M918L/T or L1014F mutations were detected, these mutations are widely present in other thrips closely related to the *M. usitatus*, indicating potential risks that may arise in the future. Currently, T929I is the sole mutation associated with pyrethroid resistance identified in the *M. usitatus* in Hainan, and its decreasing frequency may be linked to novel resistance adaptations within the VGSC of this insect. The findings of this study provide a theoretical foundation for the early monitoring and scientific management of resistance in the *M. usitatus* in Hainan.

Citation: Xia G, Yuan D, Wang L, Gao R, Wang Q, et al. 2026. Evolutionary dynamics of pyrethroid resistance in the *Megalurothrips usitatus* of Hainan and detection of voltage-gated sodium channel mutation sites. *Tropical Plants* 5: e011 https://doi.org/10.48130/tp-0026-0010

Introduction

The *Megalurothrips usitatus*, belonging to the family Thripidae (Thysanoptera), is a devastating pest of leguminous crops in tropical and subtropical regions. Its host range includes economically important legumes such as cowpea (*Vigna unguiculata*) and common bean (*Phaseolus vulgaris*). This pest is characterized by its broad host range adaptability, diverse modes of damage, and rapid evolution of pesticide resistance, making it a critical factor that limits the production of high-quality, high-yield legume crops[1–3]. Both adult and nymphal stages of *M. usitatus* feed on host flowers, tender leaves, and young fruits, utilizing their scraping-sucking mouthparts. Through abrading the plant epidermis and extracting cellular fluid, they directly undermine the structural integrity and physiological functionality of photosynthetic tissues, thereby inducing silvery-white scarring on leaves, chlorophyll degradation, and substantial reduction of photosynthetic capacity[4,5]. Damage to floral structures frequently precipitates petal deformation and pollination failure, whereas feeding on young fruitlets results in persistent pitting or fruit deformation, including pod curvature and surface roughening in cowpea. Consequently, severe damage is inflicted on cowpea crops, resulting in a significant decline in quality[6–8]. Furthermore, this insect exhibits diminutive body dimensions, with adults measuring approximately 1.5–2.0 mm and nymphs merely 0.8–1.2 mm in length. The species demonstrates pronounced thigmotaxis and frequently conceals itself within the floral structures of leguminous plants, encompassing pistils and petal folds, as well as beneath the calyx of young fruitlets[9]. This ecological behavior considerably exacerbates the difficulty of field control. Cowpea, a leguminous vegetable esteemed for its palatability and nutritional value, occupies considerable importance in human dietary patterns. Hainan Province, situated in tropical regions and characterized by the absence of winter, abundant solar radiation, and copious precipitation, provides environmental conditions exceptionally favorable for cowpea cultivation. Consequently, cowpea has become an essential cash crop vital to the economic livelihoods of local farming communities[10,11]. The intensification of large-scale cowpea production in Hainan has, however, provided *M. usitatus* with a stable and conducive habitat for population proliferation. This development has correspondingly precipitated a substantial escalation in chemical insecticide dependence. Historically, pyrethroid insecticides—specifically permethrin and deltamethrin—have been extensively deployed against *M. usitatus* owing to their superior efficacy and relatively benign mammalian toxicity profiles. However, the rate of resistance development in this pest population has considerably surpassed initial projections[12–15].

Voltage-gated sodium channels (VGSCs) are extensively distributed throughout the nervous systems of both vertebrate and invertebrate organisms, serving as fundamental molecular substrates for the transduction of electrical signals within nerve cells. The functional integrity of these channels directly determines the fidelity and efficiency of neuronal signal propagation[16]. As specialized membrane protein channels possessing critical physiological roles, VGSCs additionally constitute the principal target site for

various animal-derived neurotoxins, encompassing tetrodotoxin, scorpion toxins, and batrachotoxin[17]. Moreover, they function as the primary molecular targets of classical insecticides, including pyrethroids and dichlorodiphenyltrichloroethane (DDT)[18]. The α-subunit comprises four homologous domains (Domains I–IV), each containing six transmembrane segments (S1–S6). Among these transmembrane segments, the S4 segment functions as the voltage sensor, whereas the S5–S6 segments collectively constitute the ion-conducting pore of the channel[19–21]. Pyrethroid insecticides exert their insecticidal activity by binding to two distinct regions within the VGSC[22,23]. This binding interaction destabilizes the channel's open conformation, suppresses channel inactivation, and consequently permits sustained sodium ion influx. The resultant perturbation of neuronal electrical signaling ultimately produces paralysis and lethality in insects[24,25]. Amino acid substitutions within the sodium channel can alter its three-dimensional architecture, thereby reducing the binding affinity of pyrethroids to their target site. This mechanistic basis of resistance is designated as knockdown resistance (kdr). Presently, numerous kdr mutations conferring elevated resistance levels have been identified across diverse insect species, with these mutations predominantly concentrated within Domains II and IV of the VGSC[26,27].

Pyrethroid insecticides represent synthetic derivatives produced through chemical modification of bioactive constituents derived from natural pyrethrins. According to the presence or absence of an α-cyano group within their molecular structure, they are categorized into two distinct classes: Type I pyrethroids, lacking an α-cyano group, exemplified by permethrin, bifenthrin, etc.; and Type II pyrethroids, containing an α-cyano group, represented by deltamethrin and λ-cyhalothrin, etc[28,29]. Empirical evidence demonstrates that Type I pyrethroids exert their toxic effects by binding to specific sites on channel proteins, disrupting normal transmembrane sodium ion transport, and eliciting repetitive electrical discharge (i.e., repetitive firing) in nerve axons. This aberrant electrophysiological activity precipitates sustained hyperexcitation of presynaptic nerve terminals, ultimately disrupting synaptic signal transmission[30]. Although both types of agents target VGSCs, the toxicological mechanisms of type II pyrethroids differ significantly from those of type I. Type II pyrethroids do not induce repetitive firing in neural tissues; instead, they prolong the duration of sodium currents. This prolongation results in sustained depolarization of the cell membrane, which hinders the generation and conduction of normal action potentials, thereby disrupting synaptic physiological function[20]. Mutations in VGSC conferring knockdown resistance (kdr) represent a principal focus of contemporary research in the field of insecticide resistance mechanisms[31]. Grounded in this mechanistic foundation, detection of kdr mutation frequencies at specific loci within insect VGSCs enables inference of the proportion of resistant individuals within a population, thereby facilitating indirect assessment of population-level resistance status and providing a molecular technical framework for early detection of insecticide resistance development[32].

Based on the above research background, this investigation seeks to elucidate the resistance evolution dynamics of *M. usitatus* in Hainan Province toward pyrethroid insecticides through systematic mutation site detection and resistance level assessment conducted over three consecutive years. Furthermore, by characterizing the complete-length VGSC gene sequence of this species and identifying resistance-associated mutation sites, the molecular mechanism underlying resistance formation is further clarified. By delineating the resistance evolution trajectory of *M. usitatus* to pyrethroids, this research endeavors to provide a theoretical framework and practical guidance for the scientifically-informed formulation of insecticide rotation strategies, judicious insecticide application, and retardation of resistance progression in field populations.

Materials and methods

Test insects and chemical reagents

The susceptible strain (HK-S) was collected from Yunnan and reared on fresh cowpea without pesticide residues. Four field populations, designated as CM-R (CM2024, CM2025, CM2026), LD-R (LD2024, LD2025, LD2026), SY-R (SY2024, SY2025, SY2026), and LS-R (LS2024, LS2025, LS2026), were collected from Chengmai County, Ledong Li Autonomous County, Sanya City, and Lingshui Li Autonomous County, Hainan Province, China, between 2024 and 2026, respectively; detailed geographic coordinates are provided in Table 1. The susceptible strain (HK-S) was collected from Yunnan and reared on fresh, pesticide-free cowpea. All tested insect sources were reared under artificial climate conditions set at a temperature of 26 ± 1 °C, a relative humidity of 65% ± 5%, and a photoperiod of 16:8 h (light : dark); these rearing conditions were maintained from 2019 to 2025. The tested insecticides were as follows: deltamethrin (purity 100%), bifenthrin (purity 100%), and cypermethrin (purity 100%), all purchased from Beijing J&K Scientific Ltd (Beijing, China).

Bioassay

Technical-grade insecticides were initially dissolved in acetone to prepare stock solutions, and subsequently diluted with 0.1% Triton X-100 solution (Sigma, USA). Six to eight concentration gradients were established for each insecticide, and each concentration was tested with three mechanical replicates. In this study, bioassays against *M. usitatus* were conducted using the residual film method, with the detailed procedure described as follows: Pre-treatment of experimental materials: Fresh, pesticide-free cowpea pods were selected; only those with a diameter suitable for insertion into 1.5 mL centrifuge tubes were chosen. The selected pods were rinsed, air-dried, and cut into 0.6–0.8 cm segments. A 20-mesh insect-proof screen was cut into rectangles of approximately 2.5 cm per side and set aside. Chemical treatment: The pre-treated cowpea segments and insect-proof net pieces were immersed together in the corresponding insecticide solution for 5 min. They were then removed with disposable forceps, placed on absorbent paper, and air-dried in a fume hood. Additional 1.5 mL centrifuge tubes were prepared; a hole was drilled through the center of each tube cap with a high-temperature electric soldering iron to ensure air exchange. For each concentration, 1.5 mL of the corresponding insecticide solution was added to the tubes. After 1 h of soaking, the

Table 1. Field collection information table of *M. usitatus*.

Strains	Collection site	Year	Longitude and latitude	Host
CM-R	Chengmai County, Hainan Province	2024–2026	N 20°20'31", E 110°30'11	Cowpea
LD-R	Ledong Li Autonomous County, Hainan Province	2024–2026	N 18°40'03", E 109°30'25"	Cowpea
SY-R	Yazhou District, Sanya City, Hainan Province	2024–2026	N 18°23'05", E 109°9'44"	Cowpea
LS-R	Lingshui Li Autonomous County, Hainan Province	2024–2026	N 18°31'42", E 110°1'35"	Cowpea

solution was discarded, and the tubes were drained of residual liquid and air-dried. Insect inoculation: Using a laboratory-patented aspirator, adults of the laboratory-reared susceptible strain and field-collected adults were separately transferred into the insecticide-treated centrifuge tubes. Each tube received 25 adults. Subsequently, the insecticide-treated cowpea segments were added, and the 20-mesh netting was finally secured with the tube cap to prevent the escape of test insects. The inoculated centrifuge tubes were placed horizontally in a controlled climate chamber set at 25 °C, 70% relative humidity, and a photoperiod of 16 h light : 8 h dark (L : D). Data recording and analysis: Adult mortality in each treatment group was scored 48 h after insecticide exposure. Statistical analysis of the experimental data was performed using PoloPlus 2.0 software.

Cloning of the VGSC gene from *M. usitatus*

Total RNA was extracted from adult *M. usitatus* using Trizol® Reagent (Ambion, USA) and reverse transcribed into cDNA with the PrimeScript™ II 1st Strand cDNA Synthesis Kit (TaKaRa, Japan). Specific primers $MuNa_v$-5(F)/3(R) (synthesized by Tsingke, Beijing, China; sequences are listed in Table 2) were designed, and the full-length VGSC gene was amplified using cDNA as the template. PCR products were examined by 1% agarose gel electrophoresis, purified and recovered using an Omega Bio-Tek kit (USA), ligated into the PGH19 vector, and then transformed into XL-10-gold competent cells (Biomed, Beijing, China). Following 90 min of shaker incubation, the cells were spread onto LA plates containing 10 mg/mL ampicillin and incubated inverted for 24 h. Single colonies were picked and subjected to colony PCR to eliminate false positives. Positive clones were then cultured for amplification, and plasmids were extracted using an Omega kit (USA). The extracted plasmids were verified by restriction digestion with Hind III-HF enzyme (NEB, Beijing, China) and subsequently sent to Tsingke Biotechnology Co., Ltd for sequencing.

Genotyping of pyrethroid resistance-associated mutations

Thirty adults of *M. usitatus* were selected from each of the five populations (HK-S, CM-R, LD-R, SY-R, and LS-R), and genomic DNA was individually extracted from each adult using a DNA extraction kit (Beijing Biotech). Specific primers, Domain II-5(F) and Domain II-3(R) (synthesized by Tsingke, Beijing, China), were designed to target the Domain II region of the VGSC gene. PCR amplification was performed using Vazyme Rapid Taq Master Mix. The PCR products were purified and recovered using an Omega kit (USA), ligated into the Vazyme T-vector, and transformed into StBl2 competent cells. After 90 min of incubation with shaking, the cells were spread onto LA solid medium plates containing 10 mg/mL ampicillin and incubated inverted for 24 h. Single colonies were picked and subjected to colony PCR for verification. Positive clones were cultured for amplification and then sent to Tsingke Biotechnology Co., Ltd for sequencing. The obtained sequencing data were analyzed using DNASTAR Lasergene V7.1 Editseq software, and the frequency of the target mutation sites was calculated.

Results

Resistance level of *M. usitatus*

Using the residual film method, the toxicity of three pyrethroids against the susceptible strain (HK-S) and four field populations (CM-R, LD-R, SY-R, LS-R) of *M. usitatus* was consecutively determined over three years; the results are presented in Tables 3–5. The bioassay results from 2024 indicated that the CM-R strain exhibited the highest resistance, with maximum LC_{50} values of 4,642.120, 2,489.687, and 2,380.572 mg/L for the three insecticides, respectively. The SY-R and LS-R strains followed, with maximum LC_{50} values of 3,602.825, 2,049.838 mg/L, and 2,459.628 mg/L and 2,999.842, 2,699.051 mg/L, and 3,652.185 mg/L, respectively. The LD-R strain showed comparatively weaker resistance, yet its levels remained higher than those of HK-S, with maximum LC_{50} values of 2,710.853, 2,579.637, and 2,461.168 mg/L.

Compared with 2024, the resistance levels of the four geographical populations to deltamethrin, bifenthrin, and cypermethrin all increased in 2025. The LC_{50} values of the four populations against deltamethrin were 3,181.355, 3,102.792, 2,583.096, and 3,276.117 mg/L, respectively. Against bifenthrin, the LC_{50} values were 5,154.927, 3,508.291, 4,127.643, and 3,601.884 mg/L, respectively. For cypermethrin, the LC_{50} values were 3,342.027, 3,055.231, 2,963.782, and 4,102.857 mg/L, respectively. In 2026, resistance to the three pyrethroids continued to increase in the four field populations, albeit at a decelerated rate, and differential resistance patterns were observed. For deltamethrin: LD-R and LS-R exhibited the highest resistance (LC_{50} = 3,573.267 and 3,553.753 mg/L, respectively), followed by CM-R and SY-R (LC_{50} = 3,302.052 and 2,962.999 mg/L, respectively). For cypermethrin: SY-R and LD-R displayed comparable resistance levels (LC_{50} = 3,359.198 and 3,319.287 mg/L, respectively), while LS-R exhibited higher resistance than CM-R (LC_{50} = 4,314.532 and 3,738.598 mg/L, respectively). For bifenthrin: LD-R and LS-R exhibited comparable resistance (LC_{50} = 3,964.617 and 3,946.913 mg/L, respectively); CM-R possessed the highest resistance (LC_{50} = 5,222.599 mg/L), followed by SY-R (LC_{50} = 4,440.504 mg/L). Based on three consecutive years of resistance monitoring, significant selectivity differences were observed among geographical populations in response to distinct insecticides. The relative resistance ranking of the four field populations to the three pyrethroid insecticides was bifenthrin > cypermethrin > deltamethrin. The overall resistance levels of the four geographical populations to the three tested pyrethroid insecticides were ranked as follows: CM-R > LS-R > SY-R > LD-R (Fig. 1).

SNP/INDEL analysis of pyrethroid resistance-associated mutations

To assess potential sequence variations among different geographical populations of *M. usitatus* and the selected strains for pesticide screening, this study cloned and validated the integrity and correctness of the VGSC gene $MuNa_v$1-1 of *M. usitatus* from the experimental population. The sequence exhibited complete

Table 2. Primers for the full-length application and mutation frequency detection of VGSC in *M. usitatus*.

Primer name	Primer sequence	Usage
$MuNa_v$-5(F)	TTGGCAGTCAATTCCCCGGGGCCACCATGCCGAGTGTCCGGGAGTCG	Full-length cloning of VGSC
$MuNa_v$-3(R)	AGTCGTAACCAGATCAAGCTTTCAGACATCCGCAAGGGCCGGAG	
Domain II-5(F)	ACATTTTCTGCGTGTGGGACTGC	Detection of mutation sites in Domain II
Domain II-5(R)	CCAGTTGATAAATCGTGATATTC	

Table 3. Resistance levels of *M. usitatus* to Deltamethrin.

Treatment	Strain	Sample No.	Slope ± standard error	Degree of freedom	Chi-square	LC_{50} (95% confidence interval)	Resistance ratio
Deltamethrin	HK-S	444	1.975 ± 0.239	4	0.279	8.148 (5.853–10.311)	1
	CM2024	461	2.545 ± 0.016	4	4.864	2,489.687 (1,473.860–4,688.216)	305.6
	CM2025	450	5.197 ± 0.571	4	0.173	3,181.355 (2,890.989–3,514.066)	390.4
	CM2026	449	3.920 ± 0.433	4	0.210	3,302.052 (2,945.182–3,755.924)	405.3
	LD2024	445	1.162 ± 0.133	4	7.676	2,579.637 (2,469.245–3,151.628)	316.6
	LD2025	441	1.096 ± 0.217	4	3.294	3,102.792 (1,902.736–5,426.599)	380.8
	LD2026	450	2.947 ± 0.329	4	0.091	3,573.267 (3,090.145–4,270.751)	438.6
	SY2024	438	0.905 ± 0.127	4	0.890	2,409.838 (1,472.794–3,195.164)	295.8
	SY2025	446	1.477 ± 0.073	4	1.011	2,583.096 (1,401.633–5,023.782)	317.0
	SY2026	447	3.102 ± 0.308	4	1.268	2,962.999 (2,131.597–4,757.661)	363.6
	LS2024	443	2.190 ± 0.169	4	3.672	2,699.051 (2,730.686–2,857.614)	331.3
	LS2025	440	2.174 ± 0.228	4	1.806	3,276.117 (1,396.584–6,403.851)	402.1
	LS2026	448	2.952 ± 0.316	4	1.281	3,553.753 (2,280.381–4,217.518)	436.2

Resistance fold = Field population LC_{50}/Sensitive strain (HK-S) LC_{50}. HK-S is an indoor strain that has not been exposed to insecticides for an extended period, specifically from 2019 to 2025, and its LC_{50} serves as the fixed benchmark for all comparisons.

Table 4. Resistance levels of *M. usitatus* to Bifenthrin.

Treatment	Strain	Sample No.	Slope ± standard error	Degree of freedom	Chi-square	LC_{50} (95% confidence interval)	Resistance ratio
Bifenthrin	HK-S	444	2.248 ± 0.293	4	0.461	7.610 (5.501–9.515)	1
	CM2024	446	0.810 ± 0.120	4	2.060	4,642.120 (2,744.790–5,345.450)	610.0
	CM2025	445	2.746 ± 0.386	4	0.704	5,154.927 (4,253.658–6,853.767)	677.4
	CM2026	450	2.233 ± 0.291	4	0.461	5,222.599 (4,167.747–7,257.130)	686.3
	LD2024	441	0.713 ± 0.124	4	0.154	2,710.853 (1,747.671–5,465.877)	356.2
	LD2025	429	1.541 ± 0.155	4	1.045	3,508.291 (2,491.721–7,786.022)	461.0
	LD2026	449	3.409 ± 0.416	4	0.428	3,964.617 (3,461.532–4,705.489)	521.0
	SY2024	438	0.801 ± 0.129	4	0.025	3,602.825 (2,246.790–7,576.970)	473.4
	SY2025	430	1.206 ± 0.022	4	2.964	4,127.643 (2,578.660–7,906.107)	542.4
	SY2026	448	3.059 ± 0.397	4	0.495	4,440.504 (3,790.218–5,507.876)	583.5
	LS2024	446	2.902 ± 0.222	4	7.844	2,999.842 (2,771.627–3,289.249)	394.2
	LS2025	450	1.794 ± 0.067	4	2.454	3,601.884 (2,391.087–6,201.144)	473.3
	LS2026	449	4.741 ± 0.580	4	4.453	3,946.913 (3,371.774–4,824.179)	518.7

Resistance fold = Field population LC_{50}/Sensitive strain (HK-S) LC_{50}. HK-S is an indoor strain that has not been exposed to insecticides for an extended period, specifically from 2019 to 2025, and its LC_{50} serves as the fixed benchmark for all comparisons.

Table 5. Resistance levels of *M. usitatus* to Cypermethrin.

Treatment	Strain	Sample No.	Slope ± standard error	Degree of freedom	Chi-square	LC_{50} (95% confidence interval)	Resistance ratio
Cypermethrin	HK-S	447	1.730 ± 0.222	4	0.566	6.756 (4.387–9.029)	1
	CM2024	425	2.871 ± 0.062	4	2.524	2,380.572 (1,209.860–4,688.216)	352.4
	CM2025	450	2.102 ± 0.219	4	0.425	3,342.027 (2,773.125–4,222.895)	494.7
	CM2026	450	1.651 ± 0.179	4	0.081	3,738.598 (2,939.492–5,142.503)	553.4
	LD2024	445	2.203 ± 0.187	4	1.724	2,461.168 (2,390.935–2,937.372)	364.3
	LD2025	445	2.017 ± 0.884	4	1.027	3,055.231 (1,491.087–4,923.077)	452.2
	LD2026	450	2.250 ± 0.262	4	2.250	3,319.287 (2,828.367–4,040.714)	491.3
	SY2024	437	0.866 ± 0.125	4	0.816	2,459.628 (1,644.078–4,515.853)	364.1
	SY2025	429	2.151 ± 0.017	4	1.739	2,963.782 (1,708.851–4,996.745)	438.7
	SY2026	448	2.970 ± 0.319	4	1.205	3,359.198 (2,913.821–3,984.137)	497.2
	LS2024	441	0.891 ± 0.125	4	0.939	3,652.185 (2,219.346–8,724.188)	540.6
	LS2025	448	2.966 ± 0.693	4	1.831	4,102.857 (3,201.822–7,012.696)	607.3
	LS2026	449	3.874 ± 0.509	4	0.535	4,314.532 (3,795.844–5,094.333)	638.6

Resistance fold = Field population LC_{50}/Sensitive strain (HK-S) LC_{50}. HK-S is an indoor strain that has not been exposed to insecticides for an extended period, specifically from 2019 to 2025, and its LC_{50} serves as the fixed benchmark for all comparisons.

alignment with the reference sequence (accession number MZ043856)[5], suggesting that this gene is highly conserved within the experimental population. Consequently, it can be employed for subsequent detection of resistance mutations and functional verification. After obtaining the full-length gene of the VGSC from the *M. usitatus*, a 3D simulation of the VGSC was constructed based on its basic structure and amino acid sequence information (Fig. 2).

Additionally, 30 adult *M. usitatus* were selected from each of the five populations: HK-S, CM-R, LD-R, SY-R, and LS-R. Their individual DNA was used as a template for cloning the VGSC structure Domain II region using RT-PCR technology. During the analysis, special attention was paid to the super kdr mutation site M918T, which has not been reported in *M. usitatus*, as well as the kdr mutations L1014F and M918L reported in *Thrips tabaci*. The sequencing data identification results (Table 6) showed that M918T/L and L1014F were not

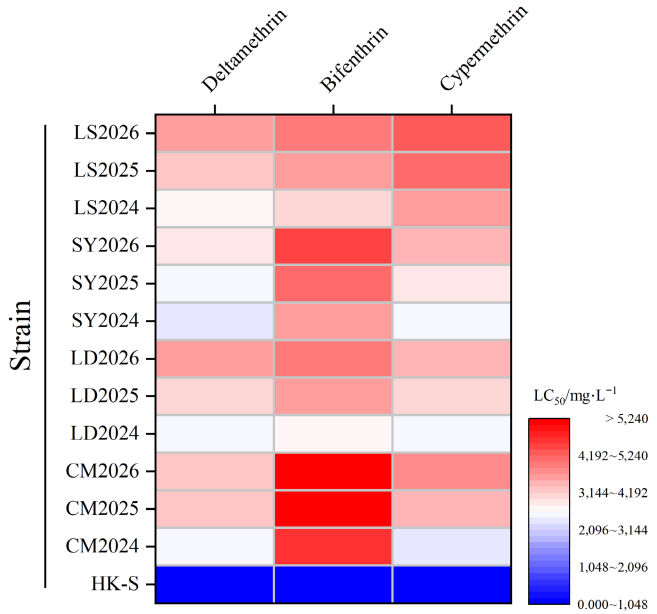

Fig. 1 2024–2026 resistance levels of *M. usitatus* strains.

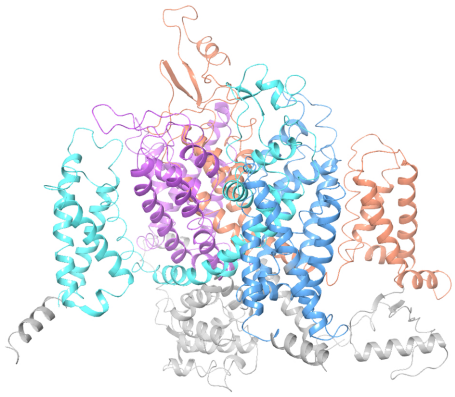

Fig. 2 3D model of *M. usitatus* VGSC (orange area: Domain I, blue area: Domain II, light blue area: Domain III, purple area: Domain IV).

detected in the tested populations. However, the reported T929I mutation was detected in all populations except for the sensitive strain HK-S, which is located in the VGSC Domain II (Table 7, Fig. 3).

Compared to the sensitive strain HK-S, the T929I mutation was detected in all four field populations (CM-R, LD-R, SY-R, LS-R) across all years, whereas the frequency of this mutation was zero in HK-S, with no detection of this mutation. In 2024, the T929I mutation frequency in all four field populations reached 100%, representing the highest mutation frequency detected at this locus. In 2025, the mutation frequency at this locus began to differentiate among populations, with LD2025 and SY2025 maintaining a 100% mutation frequency, while the mutation frequency in CM2025 decreased to 93.3%, and that in LS2025 decreased to 90.0%. In 2026, the T929I mutation frequency in all four field populations showed varying degrees of decline. The mutation frequency in CM2026 further decreased to 90.0%, while that in LD2026 and SY2026 both decreased to 96.7%. LS2026 maintained the same mutation frequency of 90.0% as in 2025. Overall, from 2024 to 2026, the T929I mutation frequency in the four field populations showed a decreasing trend from the initial 100% year by year, with no increase in mutation frequency observed. Furthermore, the differentiation in mutation frequency among populations began to emerge in 2025 and continued to persist in 2026 (Table 6).

Discussion

In agricultural production practices, diverse pesticides are extensively utilized for managing crop diseases and arthropod pests, thereby providing essential support for sustaining food production. However, with the continuous escalation of pesticide applications, target pests have progressively developed resistance globally, presenting a formidable challenge to the Integrated Pest Management (IPM) system worldwide[33,34]. Pyrethroid insecticides, representing the second most extensively used class of commercial insecticides globally, are deployed to control arthropod pests in agricultural and urban environments[35]. Their application is particularly prevalent in tropical and subtropical regions, where pest outbreaks occur with high frequency.

Hainan Province exhibits a typical subtropical climate characterized by year-round warmth and moisture, conditions that facilitate the proliferation and reproduction of insect pests. This ecological setting leads to severe overlapping generations and consequently accelerates the development of insecticide resistance and complicates pest management efforts. Previous investigations have demonstrated that field populations of *M. usitatus* collected from Haikou, Chengmai, Ledong, and Sanya in Hainan Province exhibit substantial resistance to β-cypermethrin and bifenthrin[36], a pattern further corroborated by the resistance monitoring data presented in this study. Between 2024 and 2025, resistance of *M. usitatus* to

Table 6. Mutation frequency of *M. usitatus* M918L/T, L1014F, and T929I mutation sites.

Strain	Year	M918L	Mutation frequency	M918T	Mutation frequency	T929I	Mutation frequency	L1014F	Mutation frequency	Total samples
HK-S	2025	M/L	0	M/T	0	T/I	0	L/F	0	29
CM2024	2024	M/L	0	M/T	0	T/I	100	L/F	0	29
CM2025	2025	M/L	0	M/T	0	T/I	93.3	L/F	0	30
CM2026	2026	M/L	0	M/T	0	T/I	90.0	L/F	0	30
LD2024	2024	M/L	0	M/T	0	T/I	100	L/F	0	30
LD2025	2025	M/L	0	M/T	0	T/I	100	L/F	0	30
LD2026	2026	M/L	0	M/T	0	T/I	96.7	L/F	0	30
SY2024	2024	M/L	0	M/T	0	T/I	100	L/F	0	29
SY2025	2025	M/L	0	M/T	0	T/I	100	L/F	0	28
SY2026	2026	M/L	0	M/T	0	T/I	96.7	L/F	0	30
LS2024	2024	M/L	0	M/T	0	T/I	100.0	L/F	0	29
LS2025	2025	M/L	0	M/T	0	T/I	90.0	L/F	0	30
LS2026	2026	M/L	0	M/T	0	T/I	90.0	L/F	0	30

To ensure the reliability and accuracy of the experimental data, samples that did not meet quality standards were excluded from the final statistical analysis.

Table 7. Amino acid sequences of the Domain II-localized T929I mutation and the pyrethroid-binding site (IIL45-IIS5-IIIS6) in *M. usitatus*.

Channel	Segment					
$MuNa_v1$-1	IL45-S5	[252]VPGLKTIVGA	VI	ESVKNLRDVI	ILTMFSLSVF	ALMGLQIY
	IIL45-S5	[934]WPTLNLLISI	MG	RTMGALGNLT	FVLCIIIFIF	AVMGMQLF
	IIIL45-S5	[1431]MQGMRVVVNA	LV	QAIPSIFNVL	LVCLIFWLIF	AIMGVQLF
	IVL45-S5	[1749]AKGIRTLLFA	LA	MSLPALFNIC	LLLFLVMFIF	AIFGMSFF
	IS6	[402]PWHMLFFIVI	IFLGSFYLVN	LILAIVAMSY	DE	
	IIS6	[1025]WSCIPFFLAT	VVIGNLVVLN	LFLALLLSNF	GS	
	IIIS6	[1552]IYMYLYFVFF	IIFGSFFTLN	LFIGVIIDNF	NE	
	IIIS6	[1852]TIGITFLLSY	LVISFLIVIN	MYIAVILENY	SQ	

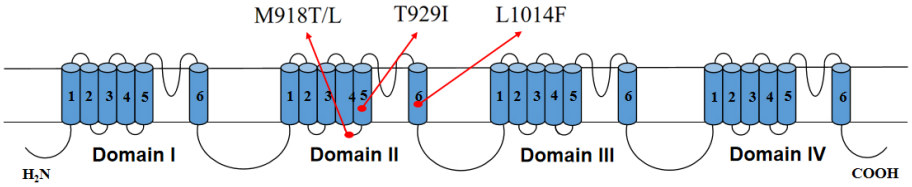

Fig. 3 Topological structure diagram of the VGSC M918L/T, T929I and L1014F mutation sites in the *M. usitatus*.

pyrethroid insecticides escalated rapidly. The 2024 bioassay revealed an LC_{50} value of 2,489.687 mg/L for the CM2024 population, which increased to 3,181.355 mg/L in 2025, representing a notable elevation. The resistance ratio rose from 305.6-fold to 390.4-fold within a single year. Concurrently, the LC_{50} for bifenthrin reached 5,154.927 mg/L (CM2025), indicating a 1.1-fold increase relative to 2024 and a 45-fold increase relative to 2015[14]. Furthermore, *M. usitatus* exhibited differential susceptibility among various pyrethroid compounds, with the highest resistance level observed against bifenthrin, followed by cypermethrin, and the lowest against deltamethrin. We hypothesize that this phenomenon may arise from the varying binding affinities and mechanisms associated with the molecular structures and target sites of different insecticides. Furthermore, disparities in the activity of metabolic detoxifying enzymes among distinct populations may also influence drug selectivity. This hierarchy provides a reference framework for optimizing future field applications of pyrethroid insecticides.

Insects primarily circumvent the toxic effects of insecticides through detoxifying enzyme metabolism, target-site mutations, and cuticular barrier mechanisms[37–39]. Previous research has established that pyrethroid resistance in *M. usitatus* is associated with mutations in the VGSC[40]. The M918T and L1014F substitutions, designated as 'super-kdr' and 'kdr' respectively, confer exceptionally high resistance levels across a diverse range of insect pests. Their association with resistance was initially identified in the housefly (*Musca domestica*) through molecular cloning and sequencing, and subsequently validated in an electrophysiological expression system using *Drosophila melanogaster*[41,42]. The escalating prevalence of these mutations among pest populations poses a considerable obstacle to agricultural pest management due to the extraordinarily elevated resistance level conferred[43]. Notably, thrips pests exhibit rapid reproduction rates and considerable adaptability to environmental changes. Under the selective pressure imposed by pesticides, these pests are likely to accumulate multiple mutations in VGSCs, resulting in substantial variation in mutation spectra and resistance levels across different species[44]. In *Thrips palmi* Karny, the dual mutation I265T/L1014F was initially documented in field populations in Hainan. Between 2020 and 2022, the mutation frequencies of this dual mutation in the local population (HN) increased dramatically from 53.33% to 96.67%, functional verification demonstrated that the combined mutations I265T and L1014F enhance the resistance of *T. palmi* to pyrethroid insecticides by 20 to 25 fold compared with susceptible populations[19]. In *Frankliniella occidentalis*, the mutation frequencies of L1014F vary substantially among different populations, ranging from 11.01% (Fo4) to 37.29% (Fo5)[45]. In *T. tabaci,* the M918L substitution, which is associated with high resistance in various pest species, exists in VGSCs in the heterozygous M/L form; furthermore, the dual mutation M918T/L1014F has also been documented. Notably, these two types of mutations occur exclusively in female-parthenogenetic populations of *T. tabaci*, and the M918T/L1014F dual mutation is associated with a higher adaptive cost[46].

VGSC mutations can substantially reduce the sensitivity of thrips pests to pyrethroid insecticides. In the resistant population of *M. usitatus* in Hainan, the mutation frequencies of M283R were 3.33%, 3.33%, and 10.0% from 2019 to 2021, indicating a notable upward trend[47]. As the population resistance level increased annually, the mutations T929I and K1774N emerged sequentially, with the mutation frequencies of T929I reaching 100%. Electrophysiological experiments further confirmed that these mutations confer substantial resistance to pyrethroid insecticides, including permethrin, deltamethrin, bifenthrin, and lambda-cyhalothrin in *M. usitatus*[48]. In recent years, the mutation rate of T929I has shown a slight decline in *M. usitatus* of ordinary giant thistle horses, potentially linked to fitness costs, alterations in population genetic structure, or compensatory mutations, although our study did not detect M918T and L1014F mutations, previous research on *T. tabaci* has established a strong correlation between these super kdr mutations and parthenogenesis, indicating that they may persist as low-frequency heterozygotes, even if undetected in field populations. Therefore, the distinct reproductive traits of thrips, coupled with the limitations of detection methods, imply that these mutations may still present potential risks in *M. usitatus*, further investigation is required to ascertain whether different breeding populations of *M. usitatus* will demonstrate resistance differentiation akin to that observed in whiteflies, or if the low frequency of such mutations, attributed to high fitness costs, complicates their detection[49]. From a resistance evolution perspective, the emergence of these sodium channel mutations is closely correlated with high-intensity pesticide selection pressure in agricultural fields[20]. As the overall resistance level of *M. usitatus* continues to increase, the potential risk for the emergence of M918T/L1014F dual mutations will further escalate.

This study investigated the kdr loci M918T/L, L1014F, and T929I within Domain II of the VGSC binding sites in *M. usitatus*

populations exposed to pyrethroid insecticides. No novel mutations were identified in the tested samples, with the exception of T929I. However, given the annual increase in resistance levels, we anticipate a potential risk for the emergence of M918T/L and L1014F mutations in field populations of *M. usitatus*. This concern is reinforced by the emergence of populations exhibiting exceptionally high resistance levels in closely related thrips species, including *T. tabaci*, *T. palmi* Karny, and *F. occidentalis*, which have demonstrated high resistance to pyrethroid insecticides[19,43,44]. We performed functional verification of M918T/L and L1014F utilizing the *Xenopus* oocyte expression system and the two-electrode voltage clamp technique, revealing a substantial correlation with elevated resistance of *M. usitatus* to pyrethroid insecticides (data not yet published). This finding indirectly suggests the likelihood of mutations arising when field resistance reaches a critical threshold. Such insights provide a theoretical foundation for understanding pest resistance mechanisms and inform proactive scientific prevention and control strategies. This knowledge can facilitate the design of targeted pyrethroid insecticide application strategies, including rational rotation or mixed use of compounds based on the kdr genotypes identified in field populations. Ultimately, the sustained efficacy of pyrethroid insecticides will depend on science-driven pest management approaches that prioritize comprehensive monitoring of mutation frequencies.

Conclusions

This study examined the resistance of three pyrethroid insecticides in four strains of *M. usitatus* in Hainan (CM-R, LS-R, SY-R, LD-R), and one laboratory-sensitive strain (HK-S) from 2024 to 2026. The results indicated a year-on-year increase in resistance among *M. usitatus* in Hainan Province to pyrethroid insecticides, with interannual variations in the rate of development. Notably, all strains exhibited high levels of resistance to bromoxystrobin, cypermethrin, and chlorpyrifos, with resistance levels rising sharply from 2024 to 2025 and then decelerating in 2026. The overall resistance ranking was CM-R > LS-R > SY-R > LD-R > HK-S, with cypermethrin demonstrating the highest selectivity among the pesticides tested. Additionally, mutation point detection was performed on the target sodium channel related to pyrethroid insecticides over three consecutive years. Molecular testing revealed that T929I was the sole mutation associated with pyrethroid resistance, exhibiting a change in mutation frequency among *M. usitatus* in Hainan. The mutation frequency reached 100% in 2024 but showed a population-specific decline from 2025 to 2026.

Author contributions

The authors confirm contributions to the paper as follows: methodology: Xia G, Yuan D, Wang L, Gao R, Wu S; data curation: Xia G, Yuan D, Wang L, Wang Q, Xie Y, Wayne J; resources: Wu S; draft manuscript preparation: Xia G; writing–review and editing: Wu S; supervision: Wu S; funding acquisition: Wu S. All authors reviewed the results and approved the final version of the manuscript.

Data availability

All data generated or analyzed during this study are included in this published article and its supplementary information files. The core datasets (including bioassay mortality records, LC_{50} calculation results, and mutation frequency statistics) are presented in the tables and figures of the main text, while detailed raw data and supplementary experimental records are provided in the Electronic Supplementary Information for further reference and reproduction.

Acknowledgments

This study was funded by the National Natural Science Foundation of China (Grant No. 32260666), National Key R&D Program of China (Grant No. 2024YFD1400100), HNARS2023-3-G5, the Science and Technology Commissioner Project of Hainan Province: (Grant No. KJTP202514), "111" Project (Grant No. D20024), Science and Technology special fund of Hainan Province (Grant No. ZDYF2024XDNY250).

Conflict of interest

The authors declare that they have no conflict of interest.

Supplementary information accompanies this paper online at: https://doi.org/10.48130/tp-0026-0010.

Dates

Received 21 February 2026; Revised 11 March 2026; Accepted 16 March 2026; Published online 27 March 2026

References

[1] Du C, Yang B, Wu J, Ali S. 2019. Identification and virulence characterization of two akanthomyces attenuatus isolates against *Megalurothrips usitatus* (Thysanoptera: Thripidae). *Insects* 10:168

[2] Liu P, Qin Z, Feng M, Zhang L, Huang X, et al. 2020. The male-produced aggregation pheromone of the bean flower thrips *Megalurothrips usitatus* in China: identification and attraction of conspecifics in the laboratory and field. *Pest Management Science* 76:2986–2993

[3] Mound LA, Walker AK. 1987. Thysanoptera as tropical tramps: new records from New Zealand and the Pacific. *New Zealand Entomologist* 9:70–85

[4] Zhang D, Wang R. 2024. Identification and control of *Megalurothrips usitatus*. *Vegetable* 1:81–83,85 (in Chinese)

[5] Huang W, Kon X, Ke YC, Wang S, Liu QJ, et al. 2018. Research progress on thrips *Megalurothrips usitatus* (Bagrall). *Chinese Vegetable* 2:21–27 (in Chinese)

[6] Fan Y, Tong X, Gao J, Wang M, Liu Z, et al. 2013. Spatial distribution pattern of the *Megalurothrips usitatus* on Hainan cowpea. *Journal of Environmental Entomology* 35:737–743

[7] Qiu H, Liu K, Li P, Fu B, Tang L, et al. 2014. Study on the biological characteristics of the *Megalurothrips usitatus*. *Chinese Journal of Tropical Crops* 35:2437–2441 (in Chinese)

[8] Liu K, Tang L, Li P, Han Z, Qiu H, et al. 2014. Toxicity determination of several insecticides against *Megalurothrips usitatus* and their synergistic effect after compounding. *Journal of Tropical Crops* 35:1615–1618 (in Chinese)

[9] Man Y. 2015. *Taxonomic Study of Thripini from China* (*Thysanoptera*: *Thripidae*). Thesis. Northwest A&F University, China

[10] Sun T. 2022. Current situation and development strategies of winter melon and vegetable production and marketing in Hainan. *Chinese Melons and Vegetables* 35:105–109 (in Chinese)

[11] Lv D, Lin J, Han B, Luo J, Li J. 2018. Research and application of comprehensive control techniques for pests and diseases of Hainan cowpea. *Agricultural product quality and safety* 3:35–38 (in Chinese)

[12] Tang L, Zhao H, Fu B, Han Y, Yan K, et al. 2016. Monitoring of resistance to pesticides in field populations of the *Megalurothrips usitatus* in Hainan region. *Journal of Environmental Entomology* 38:1032–1037 (in Chinese)

[13] Xiao C, Liu Y, Wu Q, Zhang Y, Wu Q, et al. 2014. Toxicity of different pesticides to cowpea thrips *Megalurothrips usitatus* (Bagnall) in Sanya area. *Plant Protection* 40:164–166 (in Chinese)

[14] Tang L, Fu B, Qiu H, Han Y, Li P, et al. 2015. Studied on the toxicity of different insecticides to against *Megalurothrips usitatus* by using a modified TIBS method. *Chinese Journal of Tropical Crops* 36:570−574 (in Chinese)
[15] Pan X, Yang L, Jin H, Lu R, Li F, et al. 2021. Research advances in occurrence and control of *Megalurothrips usitatus* in Hainan. *Chinese Journal of Tropical Biology* 12:508−513 (in Chinese)
[16] de Lera Ruiz M, Kraus RL. 2015. Voltage-gated sodium channels: structure, function, pharmacology, and clinical indications. *Journal of Medicinal Chemistry* 58:7093−7118
[17] Cestèle S, Catterall WA. 2000. Molecular mechanisms of neurotoxin action on voltage-gated sodium channels. *Biochimie* 82:883−892
[18] David MS. 2020. Neurotoxicology of pyrethroid insecticides. *Advances in Neurotoxicology* 4:113−165
[19] Wu J, Yuan L, Jin H, Zhang K, Li F, et al. 2023. Double sodium channel mutation, I265T/L1014F, is possibly related to pyrethroid-resistant in *Thrips palmi*. *Archives of Insect Biochemistry and Physiology* 113:e22021
[20] Dong K, Du Y, Rinkevich F, Nomura Y, Xu P, et al. 2014. Molecular biology of insect sodium channels and pyrethroid resistance. *Insect Biochemistry and Molecular Biology* 50:1−17
[21] Catterall WA. 2000. From ionic currents to molecular mechanisms. *Neuron* 26:13−25
[22] Du Y, Nomura Y, Satar G, Hu Z, Nauen R, et al. 2013. Molecular evidence for dual pyrethroid-receptor sites on a mosquito sodium channel. *Proceedings of the National Academy of Sciences of the United States of America* 110:11785−11790
[23] Du Y, Nomura Y, Zhorov BS, Dong K. 2015. Rotational symmetry of two pyrethroid receptor sites in the mosquito sodium channel. *Molecular Pharmacology* 88:273−280
[24] Jouraku A, Kuwazaki S, Iida H, Ohta I, Kusano H, et al. 2019. T929I and K1774N mutation pair and M918L single mutation identified in the voltage-gated sodium channel gene of pyrethroid-resistant *Thrips tabaci* (Thysanoptera: Thripidae) in Japan. *Pesticide Biochemistry and Physiology* 158:77−87
[25] Du Y, Nomura Y, Luo N, Liu Z, Lee JE, et al. 2009. Molecular determinants on the insect sodium channel for the specific action of type II pyrethroid insecticides. *Toxicology and Applied Pharmacology* 234:266−272
[26] Wang L, Lin L, Wang H, Duan W, Li F, et al. 2020. Two classic mutations in the linker-helix IIL45 and segment IIS6 of *Apolygus lucorum* sodium channel confer pyrethroid resistance. *Pest Management Science* 76:3954−3964
[27] Salgado VL, Irving SN, Miller TA. 1983. The importance of nerve terminal depolarization in pyrethroid poisoning of insects. *Pesticide Biochemistry and Physiology* 20:169−182
[28] Lund AE, Narahashi T. 1981. Interaction of DDT with sodium channels in squid giant axon membranes. *Neuroscience* 6:2253−2258
[29] Gammon DW, Brown MA, Casida JE. 1981. Two classes of pyrethroid action in the cockroach. *Pesticide Biochemistry and Physiology* 15:181−191
[30] Soderlund DM. 2012. Molecular mechanisms of pyrethroid insecticide neurotoxicity: recent advances. *Arch Toxicol* 86:165−181
[31] Mallick PK, Sindhania A, Gupta T, Singh DP, Saini S, et al. 2022. First report of classical knockdown resistance (*kdr*) mutation, L1014F, in human head louse *Pediculus humanus capitis* (Phthiraptera: Anoplura). *Medical and Veterinary Entomology* 37:209−212
[32] Chen M. 2017. *Mechanism study of pyrethroid insecticide resistance based on sodium channel mutants*. Thesis. Zhejiang University, China
[33] Popp J, Pető K, Nagy J. 2013. Pesticide productivity and food security. A review . *Agronomy for Sustainable Development* 33:243−255
[34] Cooper J, Dobson H. 2007. The benefits of pesticides to mankind and the environment. *Crop Protection* 26:1337−1348
[35] North HL, Fu Z, Metz RP, Stull MA, Johnson CD. 2023. Rapid evolution of pesticide resistance via adaptation and interspecific introgression in a major North American crop pest. *bioRxiv (Cold Spring Harbor Laboratory)* 41:129
[36] Qiu H, Fu B, Tan K, He S, Chen Z. 2022. Monitoring of resistance of field populations of *Megalurothrips usitatus* in Hainan to various insecticides. *China Plant Protection Guide* 42:67−71 (in Chinese)
[37] Broadbent AB, Pree DJ. 1997. Resistance to Insecticides in Populations of *Frankuniella Occidentalis* (Pergande) (Thysanoptera: Thripidae) from greenhouses in the Niagara Region of Ontario. *The Canadian Entomologist* 129:907−913
[38] Soderlund DM, Knipple DC. 2003. The molecular biology of knockdown resistance to pyrethroid insecticides. *Insect Biochemistry and Molecular Biology* 33:563−577
[39] Fu B, Zeng D, Liu K, Xie Y, Qiu H. 2014. Progress in the study of insecticide resistance in thrips. *Journal of Agronomy* 4:28−34 (in Chinese)
[40] Rinkevich FD, Du Y, Tolinski J, Ueda A, Wu CF, et al. 2015. Distinct roles of the $DmNa_v$ and DSC1 channels in the action of DDT and pyrethroids. *NeuroToxicology* 47:99−106
[41] Cao XM, Song FL, Zhao TY, Dong YD, Sun CX, et al. 2006. Survey of deltamethrin resistance in house flies (*Musca domestica*) from urban garbage dumps in northern China. *Environmental Entomology* 35:1−9
[42] Vais H, Williamson MS, Devonshire AL, Usherwood PN. 2001. The molecular interactions of pyrethroid insecticides with insect and mammalian sodium channels. *Pest Management Science* 57:877−888
[43] Silver KS, Du Y, Nomura Y, Oliveira EE, Salgado VL, et al. 2014. Voltage-gated sodium channels as insecticide targets. *Advances in Insect Physiology* 46:389−433
[44] Gao R, Lu R, Qiu X, Wang L, Zhang K, et al. 2023. Detection of putative mutation I873S in the sodium channel of *Megalurothrips usitatus* (Bagnall) which may be associated with pyrethroid resistance. *Insects* 14:388−388
[45] Mavridis K, Ilias A, Papapostolou KM, Varikou K, Michaelidou K, et al. 2023. Molecular diagnostics for monitoring insecticide resistance in the western flower thrips *Frankliniella occidentalis*. *Pest Management Science* 79:1615−1622
[46] Jouraku A, Tomizawa Y, Watanabe K, Yamada K, Kuwazaki S, et al. 2024. Evolutionary origin and distribution of amino acid mutations associated with resistance to sodium channel modulators in onion thrips, *Thrips tabaci*. *Scientific Reports* 14:3792
[47] Yuan L, Pan X, Lu R, Chen L, Xi Y. 2023. Monitoring of resistance to pyrethroid insecticides and detection of sodium channel mutations in Hainan *Megalurothrips usitatus*. *Plant Protection* 49:60−67 (in Chinese)
[48] Gao R, Ma S, Geng J, Zhang K, Xian L, et al. 2024. Functional characterization of double mutations T929I/K1774N in the voltage-gated sodium channel of *Megalurothrips usitatus* (Bagnall) related to pyrethroid resistance. *Journal of Agricultural and Food Chemistry* 72:11958−11967
[49] Tomizawa Y, Aizawa M, Jouraku A, Sonoda S. 2024. Field survey of reproductive modes and sodium channel mutations associated with pyrethroid resistance in *Thrips tabaci*. *Journal of Pesticide Science* 49:122−129